ISSN 2581 – 3781

AJCSE ASIAN JOURNAL OF COMPUTER SCIENCE ENGINEERING

Available Online at www.ajcse.info
**Asian Journal of Computer Science Engineering 2021;6(2):1-15**

**REVIEW ARTICLE**

# An Automatic Coronavirus Detection Systems: Survey

Ahlam Fadhil Mahmood, Saja Waleed Mahmood

*Department of Computer Engineering, University of Mosul, Mosul, Iraq*

**Received on: 01-01-2021; Revised on: 10-03-2021; Acceptance on: 01-04-2021**

## ABSTRACT

Today, the little person knows before the big the imminent danger that surrounds our world, which is the COVID-19 disease, which is caused by the coronavirus. The disease was first identified in 2019 in Wuhan, China, and has since spread globally, leading to the 2019–2020 coronavirus pandemic. Although a vaccine has been discovered for this epidemic, there is still a lot of time to ensure its end. Artificial intelligence techniques have proven themselves to be a powerful tool for automatic diagnosis of COVID-19. So far, the diagnosis of infection has been largely based on polymerase testing (polymerase chain reaction), which requires an appropriate laboratory environment and takes some time before obtaining a result. This is why it is so important to develop automatic AI-based diagnostic tools to classify the outbreak of the Coronavirus. This paper aims to provide an overview of newly developed systems based on artificial intelligence techniques that use various medical imaging methods such as computer tomography and X-rays to speed up the diagnostic process. This paper aims to inform researchers of current patient detection systems by analyzing the research according to all treatment steps and list their most important features and analyze them to build a better system through knowing the good and bad aspects of most previously research work.

**Key words:** Artificial intelligence, computer tomography, COVID-19, deep learning, X-rays

## INTRODUCTION

It is not hidden from everyone what has happened and is caused by the Corona virus since its appearance in the Chinese city of Wuhan until now, as it has changed everything in all areas and caused a major decline in the global economy. As the number of infections since the outbreak of the Coronavirus began to this day, there have been 105,805,951 confirmed cases of Covid-19, including 2,312,278 deaths.[1] Nowadays, injuries reached 107,008,664 confirmed cases, with 2,336,356 deaths and 79,015,260 recoveries as a result of COVID-19 were recorded in the world[2,3] as shown in Figure 1,the cure rate was 75.0% and the death rate was 2.9%.[1]

Symptoms of the virus are (98%) fever, (76%) cough in addition to other non-specific symptoms such as (44%) fatigue, (8%) headache, and shortness of breath.[4-6] There is an important need to recognize the disease early to avoid complications. Affected individuals are subsequently isolated to limit the spread of the disease COVID-19. First, the Chinese government the diagnosis of COVID-19 was stated to be confirmed by means of polymerase chain reaction in real-time reverse transcription polymerase chain reaction.[7] Who suffers from high negative rates in addition to the long waiting period for the result to appear in Xu *et al*., Wang, *et al*., Sethy *et al*., Narin *et al,* Rajasekaran *et al*.[8-12] Affected individuals are likely to go unnoticed and not receive adequate care in a timely fashion. Infected individuals are able to pass the virus on to peaceful individuals and it causes a real disaster. Many differences were found in chest computed tomography (CT) images in clinical studies of affected populations.[8] Therefore, computerized tomography of the chest was used as an alternative method to detect infection due to the high sensitivity caused by the emerging corona virus.[11] It was confirmed by China's National Health Commission that Chest-CT may be used to classify the infection affected by the nCoV. It is possible to use a significant quantity of pathological knowledge that can be obtained from Chest CT. There is a provision for radiologists to

**Address for correspondence:**
Ahlam Fadhil Mahmood,
E-mail: ahlam.mahmood@Gmail.com

 

scrutinize the chest CT photos. There is, therefore, a need to progress a prediction techniques focused on artificial intelligence techniques for chest CT and X-ray analysis without the involvement of a radiologist.

## Artificial intelligence

Artificial intelligence has witnessed a stimulating development over the past few years and has become an effective component in facing many of the challenges facing humanity. The last of which is Coronavirus, which has become a source of concern to the world. Intelligence is the ability of a system to get the best result against all odds. Some of them are typical situations in which there is insufficient or incomplete inputs, and some are ambiguous ones. Intelligence is that the ability to act in a way is provided to solve these difficulties.[12] Artificial intelligence is used in many areas of basic sciences, including medical and industrial. An artificial intelligence based system can be modeled on one of the below techniques: Artificial Neural Networks (ANN), Fuzzy Logic (FL), Machine Learning (ML), and Genetic Algorithm (GA) are soft computing approaches that have been creative by biological computational processes and nature's problem-solving mechanism.[13]

## ANN

ANN are a programming model that seeks to simulate the neural structure of the brain. Its widespread use eliminates many problems from simple pattern recognition tasks to advanced symbolic manipulation. An ANN is made up of a group of processing units called neurons, which are very large and interconnected by a specific topology. ANNs have the ability of learning-by-example and generalization from limited, noisy, and incomplete data. The types of ANNs are illustrated in Figure 2.

## FL

FL is a computational modeling that simulates human thinking to solve various forms of uncertainty. It enables us to convey human understanding in a linguistic way. The FL system has been used in diagnosing many diseases in many researches [14-16]. Depending on the pattern of patient data and using it to form an expert configuration system FL is capable of diagnosing many complex cases: FL System (FLC) consists of four functional blocks: (Fuzzification Interface, Knowledge Base, Decision making logic, and Defuzzification Interface) as shown in Figure 3.

## ML

It is the newer branch of the artificial intelligence shown in Figure 4 that makes the computer capable

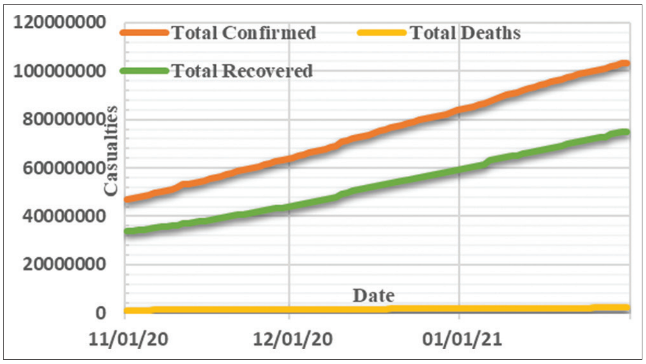


**Figure 1:** COVID-19 injuries

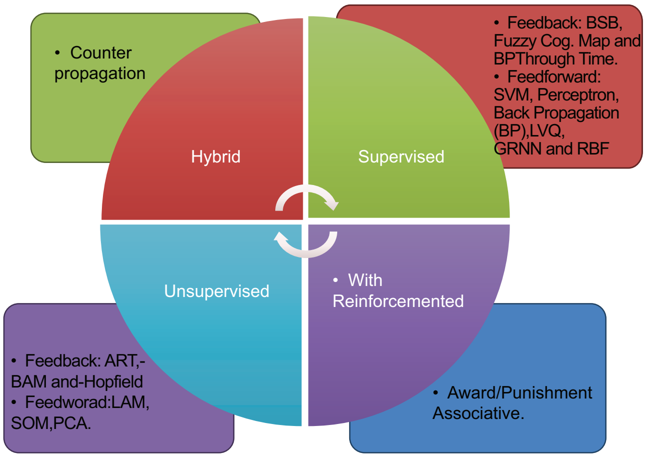


**Figure 2:** ANNs Classification according to the learning type

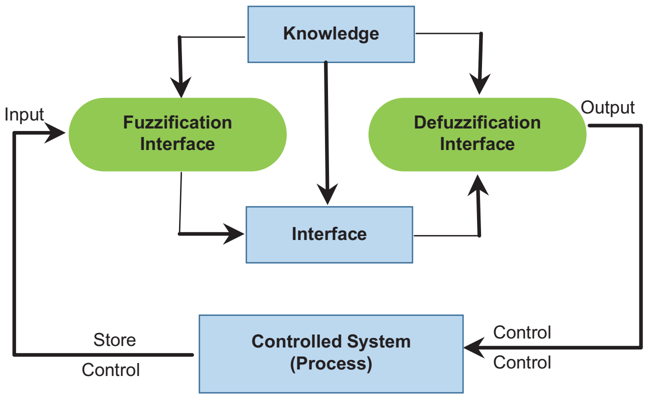


**Figure 3:** Configuration of an FLC

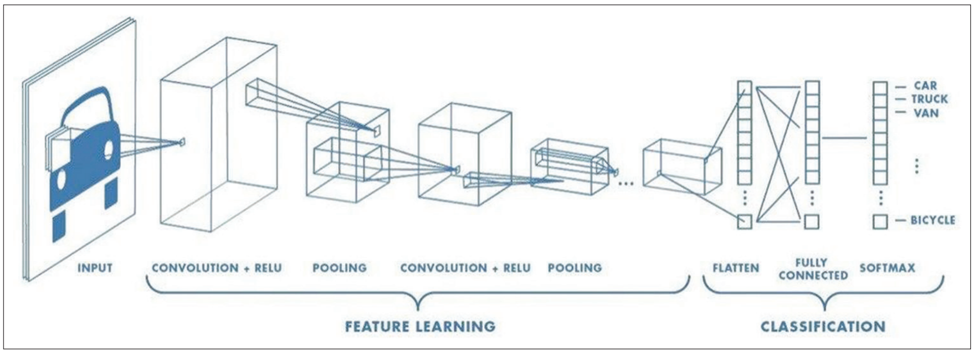


**Figure 4:** Machine learning types

of carrying out tasks and making self-decisions. Ii is one of the most effective weapons in the world in combating the spread of the coronavirus. ML algorithms are categorized into: supervised learning and un-supervised learning. In supervised learning, the availability of inputs and outputs as well as accurate predictions during training.

Once the algorithm finishes learning, what it learned can be applied to the new data, but in unattended learning, there is no need to train the algorithm for the required outputs, and instead, it uses an iterative approach called: Deep learning. Unattended learning algorithms are used for more complex processing tasks than supervised learning systems. Deep learning contains several pre-trained models that are used to diagnose many diseases including COVID-19 Such as AlexNet,[17] GoogleNe,[18] Squeeze Net,[19] various versions of the visual geometry group (VGG)[20] and various types of ResNet,[21] Xception,[22] variants from the beginning,[23] various types of MobileNet,[24] DenseNet,[25] and U-Net,[26].

## Convolutional neural network (CNN)

The CNN: CNN is a type of deep learning (Deep NN), similar to a multi-layer Perceptron network. That are commonly used in computer vision and visual field analysis; it is characterized by the presence of one or more hidden layers, which can extract the features found in images or videos, and a fully linked layer to produce the desired output.

Usually, the model architecture comprises multiple convolution layers, non-linear stimulations, set normalization, and assembling layers. Initial layers learn the lower levels concepts such as colors and edges, while later layers learn higher concepts levels such as objects.

In the lower-level, the neurons maintain information from small pieces of the image, while at the higher-level, the neurons maintain data for a larger area of the image. When more layers were added, the volume continues to decrease while the number of channels increases as shown in Figure 5.

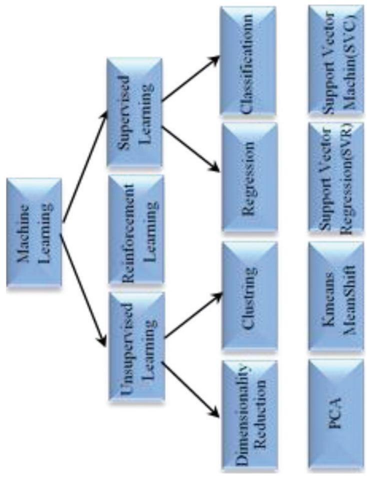


**Figure 5:** NN with many convolutional layers [27]

CNN is one of the most common and effective ways to diagnose COVID-19 from digitized images. Several reviews have been carried out to highlight recent contributions to the detection of Covid-19.[27-30]

## Computed tomography (CT) scan

It performance was examination by the X-ray technique, which works in a circular motion, related to the high performance computer to analyzing the whole image. This scrutiny permits us to notice whether any injury has occurred, or if there is a wound in an internal organ, and the exact anatomy of the patient's body can also be seen. The dimensions of the body can be observed in several vertical or horizontal sections. This type differs from normal X-ray imaging (RoentgenX-rays) which gives us a 2-dimensional image, very

**Table 1:** Image processing survey of detection Covid-19

| Ref | Type:Data(Quantity), Source | Pre-processing | Segmentation | Features | Classification Method/Layers | Tools | Results |
|---|---|---|---|---|---|---|---|
| [37] 12/03/2020 | CT slices<br>Training:270 (150N+120C)[38]<br>Testing: 157 | Image rotations, horizontal flips and cropping | U-net | - | Comprised two distinct levels:<br>(a) 3D volume analysis for nodules and focal opacities.<br>(b) 2D analysis of each slice to detect and localize larger diffuse opacities including ground glass | Use commercial off-the-shelf software | Measuring the quantitative opacity and a visualization of the larger opacities in a slice-based "heat map" or a 3D volume display |
| [39] 19/03/2020 | CXR: 25C without MERS, SARS, ARDS: GitHub(Dr. Joseph Cohen)+25N(Kaggle &Open-i)<br>Training, validation and testing ration is 60:20:20 and randomly selection for training, validation and testing in each execution | Not | Not | Layer/<br>Vector<br>Resnet50 Fc1000/1000 | A deep feature of eleven-CNN models are extracted and fed to the SVM classifier | MATLAB 2019a with DL toolbox::Acer Predator Helios 300 Core i5 8th Gen - (8 GB/1 TB HDD/128 GB SSD/ Windows 10 Home/4 GB Graphics) and equipped with NVIDIA GeForce GTX 1050T | (Resnet50 & SVM) result better Covid-19+ classification with accuracy, FPR, F1 score, MCC and Kappa: 95.38%, 6.52%, 95.52%, 91.41% and 90.76%, respectively |
| [40] 20/03/2020 | CT: 150 abdominal images (53C), from the Societa Italiana di Radiologia Medica e Interventistica | Cropped to 16x16, 32x32, 48x48, 64x64 patches | Not | GLCM, LDP, GLRLM, GLSZM, and DWT | 1. Four different patches sized (16×16, 32×32, 48×48, 64×64) with SVM<br>2. Five different feature (GLCM, LDP, GLRLM, GLSZM and DWT) extracted and were classified by SVM. With (2, 5 and 10-fold cross-validations) | N/A | Best classification accuracy (99.68%) was achieved with GLSZM feature extraction and 10-fold cross-validation. |
| [41] 24/03/2020 | CXR: 50C[GitHub(Dr. Joseph Cohen)[42]+ 50N:(Kaggle Repository).<br>Randomly split into:-<br>Training: 80%<br>Testing: 20% | Resized to 224×224 pixel | Not | No feature extraction or selection | CNN(ResNet50,Inception V3 and nceptionResNetV2) models are pre-trained through random initialization weights utilizing the Adam optimizer | Python.<br>OS done on a Google Colaboratory/Linux server with Ubuntu 16.04 OS using Tesla K80 GPU card | ResNet50 has highest training accuracy model, ResNet50 has a fast training process than (InceptionV3 and Inception-ResNetV2) models |
| [43] 03/04/2020 | CXR:1427Ds1 (224C+504N+700P))<br>Ds2(224C+504N+714 bacterial and viralP (400 bacteria+314 viraP)[44]<br>Training: N/A<br>Testing: N/A | Rescaled image to a size of 200×266 | No | Pretrained model | CNNs VGG19[45]<br>MobileNet v2[46]<br>Inception[47]<br>Xception[48]<br>Inception ResNet v2[47] | N/A | Adopted Transfer Learning procedure with CNNs.<br>MobileNet v2 and the VGG19 achieve the best classifcation accuracy over the Inception, Xception and Inception ResNet v2 CNNs<br>The training and evaluation technique was achieved with 10fold cross validation<br>Two accuracies were measured. (1) overall accuracy was distinguish to 3-classes accuracy (N-C-P) and (2) Covid-19 accuracy |

*(Contd...)*

**Table 1:** *(Continued)*

| Ref | Type:Data(Quantity), Source | Pre-processing | Segmentation | Features | Classification Method/Layers | Tools | Results |
|---|---|---|---|---|---|---|---|
| [49] 20/04/2020 | CT: 618[Ds1:219 from 110patients(mean age50Y(57.3%)male College of Medicine, Affiliated Hospital, Wenzhou Central Hospital; Zhejiang University, Ds2:224 CT from 224patients(mean age61Y(69.6%) male IAVP (H3N2, H1N1, H7N9, H5N1 and so forth, Ds3:175N (mean age 39Y(55.4%) male<br>Training:85.4%<br>Testing: 14.6% | HU threshold to binaries the resampled images<br>were raised to -200 for best filtering out the valid lung | VNet-IR-RPN[50] (256features vector) | ResNet-18 to distinguishing at least 3features: GGA, peripheral distribution on pleura, and ordinarily more than one independent emphasis of infection | ResNet[51]by concatenating the location attention in the full-connection layer to increase the total accuracy rate. | N/A<br>Intel i7-8700k(CPU) with NVIDIA(GPU) GeForce GTX 1080ti as analyzing server | Screening model to categorize images into the Covid-19, IAVP, and ITI with the corresponding confidence scores, utilizing a locality attention style<br>Overall confidence score for each CT images were evaluated by the Noisy-OR Bayesian function<br>Experimental result displayed the overall accuracy rate was (86.7%) taking all the CT cases together |
| [52] 27/04/2020 | CT: N/A<br>Training and testing dataset ratio are: 90:10%,80:20%, 60:40%, 70:30%, 40:60%, 50:50%, 20:80%, 30:70% | N/A | Multi-objective differential evolution (MODE)–based on (CNN) | CNN + ReLU+ pooling to reduce the spatial size of the convolved features[53] | Initial CNN parameters are modified using multi-objective differential evolution (MODE) | MATLAB 2019a with DL toolbox<br>Intel Core i7 with 16-GB RAM and 4GB graphics card | MODE–based on CNNs is useful for real-time classification of Covid-19 illness from the chest-CT images<br>To avoid the over fitting, 20.80-fold cross-validation were used |
| [54] 06/05/2020 | CXR485: Ds1[76C Joseph Paul Cohen dataset[55].<br>+Ds2:[219CKaggle[56] Ds[295C+65N+98P].<br>Training: 70%<br>Testing: 30% | Restructured dataset images by the Fuzzy Color strategies were stacked | No | 1000-features | DL(MobileNetV2 and SqueezeNet) and the feature sets were managed via the Social Mimic optimization (SMO). Then, features were combined and classified by SVM | Python 3.6 for the original data structure mapped by Fuzzy and heaped logic. As well as, the SMO.<br>MATLAB (2019b) for classification. Windows 10 OS(64-bit) with a 1 GB Graphics card, 4 GB Memory card, on Intel i5-Core, 2.5GHz processor | Produce faster and more precise results. 100% for Covid-19 classification and 99.27% of Normal and Pneumonia images<br>Used MobileNetV2 model, which can be simulated on mobile devices without the need to use other hospital devices |
| [57] 20/05/2020 | CXR:Ds1 (180C+42P)[58]<br>+Ds2<br>(6012P+8851N)[59]<br>Training: 83%<br>Validating: 17% | Resize: 300×300<br>Zoom Range5%<br>Horizont/Vertice flipping<br>Rotation Range (0–360°).<br>Width/Height Shifting:5%<br>Shift Range:5% | No | ResNet-18 | Xception and ResNet50V2 fold(1-5)and a concatenation of Xception and ResNet50V2 neural | N/A library on a Tesla (P100) GPU and (25GB) RAM/Google Colaboratory | CXR images are classified into three classes (N, C and P) based on Xception networks and ResNet50V2<br>Reached an average accuracy of 99.50%, and 80.53% sensitivity for the Covid-19 class, and the overall accuracy equal to 91.4% between 5-folds |

*(Contd...)*

**Table 1:** *(Continued)*

| Ref | Type:Data(Quantity), Source | Pre-processing | Segmentation | Features | Classification Method/Layers | Tools | Results |
|---|---|---|---|---|---|---|---|
| [60]<br>24/05/2020 | CXR:aligned 7nonCovid[61-67] male/female(44/36), age of 56±14.8 (55±15.6 male and 57±13.9 female)<br>Training:(88,079N+94C)<br>Testing: 153 | Resized, center cropped, rescaled | N/A | - | Used a DenseNet model[68] | Code available: https://github.com/mlmed/torchxrayvision | Single "lung opacity" output as a feature produced the best relationship(0.80), followed by four outputs(pneumonia, lung opacity, infiltration and standardization) parameters(0.79). |
| [69]<br>28/05/2020 | CXR:337Ds1: 192C[44]+5863Ds2 (142N, "Bacterial P" & "Viral P") Kaggle's<br>Training: 70%<br>Testing: 30% | 1.Resize images to :224x224 pixels<br>2.Rotation range of 20 | No | CNN Features | DL(nCOVnet-CNN) consist of 24 layers used VGG16 pre-trained[20] | N/A | Fast detect Covid-19 using nCOVnet model in 5 seconds by tune CNN hyper-parameters |
| [70]<br>17/06/2020 | 1600TEM: 16 virus: Center for Image Analysis, Uppsala University [71]+SARS-CoV–2 Infectious Diseases Rocky Mountain Laboratories and National Institute of Allergy (NIAID-RML)[72]<br>Training:80%<br>Testing:20% | Convert to grey scale) and resize to (41x41) | No | PCA for feature reduction<br>And<br>t-SNE to visualize the grouping of images | VGG16, AlexNet with SqueezeNet and NLLoss with Adam optimizer for DL styles | Python( develop DL computations/ Google Collaboratory<br>On GPU processors while PCA and t-SNE on the CPU | Results for the 16 virus types Covid-19, Astrovirus, Adenovirus, Crimean Congo hemorrhagic fever(CCHF), Dengue, Cowpox, Norovirus, Ebola, Inuenza, Lassa, Marburg, Norovirus, Papilloma, Orf, Rift, Rotavirus, West Nile and Valley]<br>Performance was evaluated by ROC curve and confusion matrix |
| [73]<br>26/06/2020 | CXR: Ds1(216C+ 1,675N) Joseph Paul in GitHub[42]1:5Y<br>Ds2: 219C+1,341N[74]40:84Y<br>Training:80%<br>Testing:20% | Rotat the image with an angle β | No | New FrMEMs,<br>a modified<br>MRFODE<br>961 features | Parallel FrMEMs on multi. coreCPU to extract features & optimization. with KNN | N/A | Parallel execution of the moment computation quickening the feature mining by a factor associated to the multi- CPU cores<br>achieved high accuracy among other DNNs procedures as compared in the paper |
| [75]<br>05/07/2020 | CXR:396[132C+132N+132P][76]<br>Training:80%<br>Testing:20% | Discard lateral and RM images histogram equalization | No | VGG-16 | TensorFlow framework with Keras, a VGG-16[45] | N/A | High sensitivity□100%, of detection COVID-19, with a high degree of specificity, areas under the curve s on identification Receiver Operating Characteristic curves are greater than 0.9 identification for the three classes |

*(Contd...)*

**Table 1:** *(Continued)*

| Ref | Type:Data(Quantity), Source | Pre-processing | Segmentation | Features | Classification Method/Layers | Tools | Results |
|---|---|---|---|---|---|---|---|
| [77]<br>18/08/2020 | CXR: Ds1: 5,828N+154C[55] and Ds2[78] | No | No | No | ResNet-101 | N/A<br>On Intel® Core™ i7-4770 CPU with GPU | More accurate ground truth for CXR-14 analysis. used airspace opacity label to develop the DL model 0.82AUC, Whereas, 1. indicates the ideal Covid-19 test<br>Increased model efficiency to 4-times by using GPU |
| [79]<br>23/08/2020 | CXR: (1583N+4292p)[80] +225C[55,58]<br>(58.8±14.9)Y and it contained 131 male and 64 female patients | Resized all images to 640×480<br>sharpening input images by a Laplacian filter (sigma = 2.5)[81] | average pixel per node (APPN) | Convolutio-nal layer by masks, split images into pre-defined dimensions for sectors utilizing filters | 38CNNexp. +10exp., 5ML, and 14(pre-trained networks) for transfer learning<br>8fold cross-validation | Ubuntu 18.01.4 LTS 64-bit OS, Intel Core i7-8700 CPU @3.20 GHz× 12, 32 GB RAM, NVidia GeForce RTX2060GPU. | A CNN without preprocessing with a minimized layer is able to detect Covid-19 in a restricted number of and in imbalanced CXR images<br>ConvNet architecture provides the highest accuracy for Covid-19 detection in CXR images |
| [82]<br>05/09/2020 | CXR:Ds1 80N(4020×4892) JSRT[83,84]+<br>Ds2:105C and 11SARS(4248× 3480)[42]<br>Training:70%<br>Testing:30% | flipping up/down and right/left, translation and rotation using<br>5-angles+Histogram modification+PCA | No | AlexNet[17]+VGG19+ GoogleNet+ResNet+SqueezeNet | Decompose, Transfer, and Compose (DeTraC) model | MATLAB 2019a on a PC with: 3.70GHz Intel(R) Core (TM) i3-6100 Duo, NVIDIA P5000GPU, 8.00GBRAM. | DeTraC with VGG19 has attained highest sensitivity 98.23%, accuracy 97.35%, and specificity of 96.34%. with (DeTraC) class decomposition. |
| [85]<br>21/09/2020 | CXR:DS1: (1675N+200C) Joseph Paul Cohen and Paul Morrison and Lan Dao[42]+<br>Ds2:Kaggle[86]+<br>Ds3:219C+1341N by SIRM[74] | Resize:224×224 | No | MPA CNN deep features | Combining Inception-CNN to extract features and a swarm(FO-MPA) to select the most relevant features | 2Environments Python3, under "Google Colab" with used TPUs, DL (Inception) and the feature extraction Matlab, for FO-MPA | IFM achieving 98.7%, 98.2%and 99.6%, 99% of accuracy and F-Score for Ds2 and Ds1<br>Selected 130, 86 out of 51 K features extracted by inception from Ds1, Ds2 |
| [87]<br>09/10/2020 | CXR:[1583N+ 675C+4275P] from Kaggle repository<br>Training:85%<br>Testing:15% | Reshape:(128x128x3) for fast processing and (256,256,3) to better performance<br>Rotation=10°<br>Horizontal Flip<br>Zoom Range=0.4 | No | Applying CNN | Inception V3/Xception Net/ ResNeXt | N/A | XCeption net provides highest accuracy (97.97%)<br>Implemented LeakyReLU activation, that helps to speed up the training and avoids the dead neurons problem |

*(Contd...)*

**Table 1:** *(Continued)*

| Ref | Type:Data(Quantity), Source | Pre-processing | Segmentation | Features | Classification Method/Layers | Tools | Results |
|---|---|---|---|---|---|---|---|
| [88] 11/11/2020 | CXR: 13,975<br>Ds1,[42] Ds2,[89]<br>Ds3(RSNA) Pneumonia,[90]<br>Ds4:ActualMed[91] Ds5:[92]<br>Training: N/A<br>Testing: N/A | cropped (top 8%) translation (±10% in X and Y), rotation (±10◦), horizontal fip, zoom (±15%) and intensity shift (±10%) | No | CNN | Covid-Net human-machine collaborative using Keras DL library with a TensorFlow back end | N/A | Covid-Net offers enhanced representational capacity and keeping computational efficiency<br>COVID-Net reaches good accuracy by obtaining 93.3% (sensitivity and positive predictive value (PPV))≥ 80% |
| [93] 03/12/2020 | CT: 349C from 216 patients+397N(MedPix, LUNA, PMC, and Radiopaedia website).<br>Training: 80%<br>Testing: 20% | Resized to 120×120 | No | Data features represent into less dimensionality before accessing the CNN | Comparison with the DenseNet-169[11] | Python on 24 Intel(R) Xeon(R) CPU E5-46070 @ 2.20GHz, 377G memory and two Quadro P2000 | Covid-CLNet accuracy equal to 91.98% testing while the highest accuracy of the comparison papers TL-CSSL is 89.1% testing accuracy |

N: Normal case, C: Corona case, MERS: Middle East respiratory syndrome, SARS: Severe acute respiratory syndrome, ARDS: Acute respiratory distress syndrome, SVM: Support vector machine, FPR: False positive rate, GLCM: Grey level co-occurrence matrix, LDP: Local directional pattern, GLRLM: Grey-level run length matrix, GLSZM: Grey-level size zone matrix, DWT: Discrete wavelet transform, Ds: Dataset, P: Pneumonia, IAVP: Influenza-A viral pneumonia, HU: Hounsfield unit, VNet-IR-RPN: Volumetric Net–inception residual network–region proposal network, GGA: Ground-glass appearance, ITI: Irrelevant to infection, ReLU: Rectified linear unit, TEM: Transmission electron microscopy, PCA: Principle component analysis, t-SEN: t-distributed stochastic neighbor embedding, NLLoss: Negative log likelihood loss, FrMEMs: Fractional multichannel exponent moments, MRFODE: Manta ray foraging optimization based on differential evolution, JSRT: Japanese Society of Radiological Technology, SIRM: Italian Society of Medical and Interventional Radiology, MPA: Marine predators algorithm, TPU: Tensor processing unit, FO-MPA: Fractional-order marine predators algorithm, RSNA: Radiological society of North America, PMC : PubMed Central, TL-CSSL: Transfer learning-contrastive self-supervised learning

**Table 2:** the comparison of references in Table 1.

| Ref | Advantages | Disadvantages |
|---|---|---|
| [37]<br>10/3/2020 | 1. Utilizes robust 2D and 3D deep learning simulations, modifying and adapting AI techniques and merging them with clinical understanding<br>2. Generating a Corona score. by evaluate progress of Covid-19 disease over time using a 3D volume review<br>3. Result: 98.2% sensitivity, 92.2% specificity | 1. In that paper time: Limited data sets as well as limited expertise in labeling and segmenting the ground-glass opacities the data specific to this new strain of the virus in humans which is very play important<br>2. Subsystem A: used in[94] software and Subsystem B: Software not declare |
| [39]<br>19/3/2020 | 1. Eleven models of CNN were tested<br>2. Accuracy, Sensitivity, and Specificity with (FPR, F1 Score, MCC, and Kappa) of various CNN models are evaluated | 1. Not used any preprocessing as resize, crop and rescale to normalized datasets, images are different as appear in their paper<br>2. Not segmented the region of interest, there is a large contrast difference of X-ray. That was drawback the classification results<br>3. Small datasets |
| [40]<br>20/3/2020 | 1. Five metrics sensitivity (SEN), specificity (SPE), accuracy (ACC), precision (PRE), and F-score are listed in four tables to verify best classification result of stage1 and stage2 with 2fold, 5fold and 10fold cross validation<br>2. Testing done for different features, patch size and three cross validations<br>3. The paper identified the best features with a specific parameter of the SVM classifier<br>4. Compared two system based on SVM with feature extraction process and without feature execration | 1. Not split datasets to train and test phase<br>2. Limited data sets<br>3. Not make any preprocessing techniques<br>4. Not mentioned to the language programed and what the implementation tools |
| [41]<br>24/3/2020 | 1. Performance results of the ResNet50 pre-training yielded the highest accuracy of 98%.<br>2. Learning rate, batch size and number of epochs experimentally set to 1e-5, 2, and 30<br>3. Results were achieved according to 5- k values (k=1-5) cross validation. | 1. Small dataset (50 COVID-19 vs. 50 Normal)<br>2. Only resize pre-processing are done<br>3. Tested only on X-ray datasets |
| [43]<br>3/4/2020 | 1. Measure the Accuracy of (2-class and 3-class), Sensitivity and Specificity<br>2. VGG19 and MobileNet v2 are the best performing CNNs results due to evaluation values (Acc.: 98.75 Sen.:92.85 and Spe.98.75) VGG19 and (Acc.: 97.40 Sen.99.10 Spe.97.09) MobileNet v2<br>3. Tabulate the parameter and description of each networks used in paper<br>4. Classify output into three classes<br>5. Experiment different parameters for transfer learning<br>6. Specify the VGG19 that achieves better accuracy | 1. Different data source, no initial treatment was mentioned<br>2. The authors did not provide details of assigning one group for training, another for testing, and a third for validation group |
| [49]<br>20/4/2020 | 1. Take at least 2 days' gap between CT datasets from the same patient to guarantee the diversity of images.<br>2. Three types of results were offered Covid-19, IAVP, with a healthy cases and summarizing their results in tables.<br>3. Reach the epoch to 1200<br>4. Used the 3D.CNN segmentation style to segment multiple candidate CT image cubes by collected the center CT image together with its 2-neighbors of each cube for advance steps.<br>5. Image patch voted to denote the entire nominee region<br>6. Detailed explanation of all the dataset information | 1. Used CT, which are more expensive than CXR images<br>2. Lack of data availability supported at that time |
| [52]<br>27/4/2020 | 1. Optimized the CNN hyper parameters by using the MODE algorithm.<br>2. Plot the Receiver Operating Characteristic (ROC).<br>3. Reveal the proposed model outperforms competitive models, CNN, ANN, and ANFIS in terms of F-measure, accuracy, specificity, sensitivity, and Kappa statistics by 2.0928%, 1.9789%, 1.6827%, 1.8262%, and 1.9276%, respectively.<br>4. Confusion matrix's was plotted of the ANN, ANFIS, CNN with the proposed algorithm | 1. The data source is not referenced in the paper<br>2. No make any preprocessing which can be improve the performance<br>3. Small datasets<br>4. Used CT images only |
| [54]<br>6/5/2020 | 1. Provides a 100% Covid-19 detecting rate by examining X-ray images<br>2. The proposed portable model can be integrated into moveable smartphone devices<br>3. Fewer parameters DL models (MobileNetV2 and SqueezeNet) compared to other deep trainings, to increase speed and time performance<br>4. Preprocessing to diminishes the interference in every image in the dataset and delivers efficient features with stacking procedure<br>5. The experimental analysis metrics: Sensitivity (Sen), Specificity (Spe.), F-score(F-Scr), Precision(Pre.), and Accuracy(Acc). True Positive(TP), False Positive(FP), True Negative(TN), and False Negative (FN) parameters of the confusion matrix were plotted with different iterations | 6. Not make resizing procedure, so if the sizes of the dataset input images are different, a complete detection triumph may not be achieved<br>7. It is still a challenge to classify very low resolution images<br>8. In accumulation plane, the sizes resolution of the original images must be equal to the organized images |

*(Contd...)*

**Table 2:** *(Continued)*

| Ref | Advantages | Disadvantages |
|---|---|---|
| [57] 20/5/2020 | 1. The average accuracy of the proposed network for detecting Covid-19 cases is 99.50%<br>2. Listed many parameters and functions used in the training phase<br>3. Confusion matrix of (concatenated network, Xception and ResNet50V2) for fold 1 and 3<br>4. Tabulate the number of true and false positives and false negatives for fold (1–5) | 1. Few images of Covid-19 among normal and pneumonia<br>2. There is an error declaring the data set<br>3. Smaller datasets from Covid-19 patients<br>4. Mistakenly identify of 68 cases as Covid-195.<br>5. Global accuracy is equal to 91.4% for 5-folds |
| [60] 24/5/2020 | 1. The proposed system has the capability to measure the militancy of the Covid-19 lung infection for the purpose of intensifying or reducing care in addition to checking treatment efficiency, especially in the intensive caring unit<br>2. Make decisions from the CXR | 1. The small number of samples precludes appropriate selection of the group and is a limitation of this study<br>2. Not making segmentation for the diseases part only, which if done will improve the system |
| [69] 28/5/2020 | 1. Provide a faster speed by identifying the features of infected patients as a fog or shadowy patches in CXRT<br>2. nCoVNet able to classify the COVID-19 patient correctly with 97.97% confidence. And 98.68% confidence to predict on a negative COVID-19 patients<br>3. Preventing data leakage by a unique patient ID<br>4. Plotting training curve of loss and Accuracy for nCOVnet models. And ROC curve for nCOVnet classifier | 1. In the discussion and conclusions medical techniques of detecting COvid-19 were written with their cost and time needed not about the medical image processing with nCOVNet<br>2. Small CXR dataset<br>3. Rotation range of 20 only<br>4. Used CXR image only |
| [70] 17/6/2020 | 1. Used 16 virus families.<br>2. The ROC plot for all DL models displayed (AUC) more than 0.9 for all virus families<br>3. Randomly selected the testing images to provide a correct prediction with relatively better probabilities<br>4. Confusion matrixes were imagined with their heat maps for all viruses<br>5. All proposed models has a larger than 0.7 accuracy (taking 2000 epochs considered)<br>6. 6.The "ensemble approach," the net outcome would order a TEM image to achieve greater accuracy than just relying on a single model | 1. The VGG16, AlexNet and SqueezeNet networks were capable to predict the classification of test images with accuracy 75.3±4.7%, 77.8±4.5% and 77.8±4.5%, respectively<br>2. Limited of the SARS-CoV–2 images (25 images only) |
| [73] 26/6/2020 | 1. Parallel implementation to accelerate the theoretical limits (×2, ×4 and ×8 for 2-, 4- and 8-multi-core)<br>2. Tabulate the time in seconds needed to extract 961 features/image (1 core (sequential), 2 cores, 4 cores and 8 cores)<br>3. MRFODE associated with other metaheuristic approaches that knowned as feature selection ways, such as MRFO, HGSO, HHO, GWO, SCA, and WOA<br>4. Tabulate the comparison outcomes according to fitness value, several nominated features, and accuracy of two datasets<br>5. Used Friedman test for each method and compared with MobileNet | 1. Images were not pre-processed<br>2. Split two data set instead of processing and merging for better classification |
| [75] 5/7/2020 | 1. Tabulate all results without and with equalization<br>2. Covid-19 class has a 100% classification results<br>3. Plot a ROC curves of each model | 1. Poor pneumonia classify(outdated of pneumonia database, omitted the current tools and some cases were captured using different magnifications<br>2. Healthy and Pneumonia classes do not have a 100% success rate<br>3. Small datasets |
| [77] 18/8/2020 | 1. The power of this paper lies in the utilize of adjudicated markers that have durable clinical relation with Covid-19 kinds and the use of jointly exclusive publicly available images for validation, training and testing<br>2. Only one nomenclature has been utilize to develop a DL- airspace opacity, that is identified to be linked to COVID-19 cases | 1. No pre-processing was done, such as standardizing or removing unwanted part from the images<br>2. No segmentation was preforming to discarded COVID-19 parts only<br>3. Sensitivity, specificity, and accuracy are 77.3%, 71.8%, and 71.9%, respectively |
| [79] 23/8/2020 | 1. Tabulate comparing result of DenseNet121, Inception V3, ConvNet#1, ConvNet#2, ConvNet#3, ConvNet#4<br>2. Sensitivity: 93.84%, specificity: 99.18%, accuracy: 98.50%, and mean ROC_AUC scores of 96.51% are reached<br>3. Enhance blurred appearance by Laplacian filter4. Comparing are done on many experiment and different classification models | 1. Results Obtained of (SVM, Logistic Reg., Decision Tree, Naive Bayes and KNN) can be improved<br>2. Results Obtained of (VGG19, VGG16, InceptionV3, MobileNet-V2, ResNet50 and DenseNet121) also can be improved |
| [82] 5/9/2020 | 1. Transform the high-dimension feature space into a lower-dimension by PCA.<br>2. Different data augmentation procedures, so flipping up/down and right/left, translation and rotation with 5-angles was added.<br>3. Histogram modification used to enhance the image contrast.<br>4. Tabulate the classification presentation n(on original and augmented test) before/after applying DeTraC, obtained by VGG19, AlexNet, ResNet, GoogleNet, and SqueezeNet in shallow case and deep tuning modes.<br>5. Ability to classify irregularities of data that are one of the most challenging in the detection of COVID-19.<br>6. Plot the accuracy curve, error and ROC analysis curve of the VGG19 model. | 1. Small dataset images<br>2. There are many other training models not tested in paper<br>3. Use of exclusive publicly available data for training, verification, and testing |

*(Contd...)*

**Table 2:** *(Continued)*

| Ref | Advantages | Disadvantages |
|---|---|---|
| [85] 21/9/2020 | 1. Select only relevant features<br>2. FO-MPA compared with WOA, HGSO, SCA, SMA, PSO, GWO, HHO, GA and basic MPA in the number of nominated features and consuming period for both datasets<br>3. The results were plotted, discussed, and the best were identified for 2Ds<br>4. Balancing amid discovery and manipulation phases and absconding from local optima were reached | 1. Pre-trained drawbacks: Inception, its architecture required large memory, storage capacity (92 M.B)<br>2. Not specify the percentage of training and testing out of the total data<br>3. Many pre-trained procedures can be test<br>4. No pre-treatment was done |
| [87] 9/10/2020 | 1. Pre-processing images on size, unified appearance and in zoom<br>2. Several convolution layers and capsules are utilizing to overcome the class-imbalance problem<br>3. Accuracy and confusion matrix matrices of Inception Xception Net, Net V3 and ResNeXt are evaluated | 1. No information about tool used to implement the algorithms<br>2. Low epochs values |
| [88] 11/11/2020 | 1. State training hyper parameters: learning rate = $2^{-4}$, epochs = 22, batch size = 64, patience = 5, factor = 0.7<br>2. Compare COVID-Net with VGG-19, ResNet-50 in architectural complexity (parameters numbers) and computational difficulty (number of multiply-accumulation [MAC]) in table<br>3. Tabulate sensitivity and PPV for COVID-Net, VGG-19, and ResNet-50 three classes<br>4. Preprocessing CXR images | 1. No information about tool used to implement the algorithms<br>2. Critical factors identified by GS Inquire often links to medical visual factors such as Ground Glass opacities, interstitial abnormalities and bilateral abnormalities that are useful for Covid-19 CXR examinations |
| [93] 3/12/2020 | 1. Weighted method based on diverse detecting matrices were used to capture boosted features<br>2. Comparing the non-compression sensing and compression sensing with three (TTT, GGG and CCC) compressing methods<br>3. Tabulate the performance comparisons in term of the (Accuracy%±std and Val_loss) of different sensing matrices at different testing samples (6.5%and10%)<br>4. Comparing the different pre-trained methods with proposed procedure | 1. The dataset is small<br>2. Apply the proposed method on CT image only rather than CXR<br>3. No preprocessing was done except resize images<br>4. Relatively lack of accuracy, especially with the adoption of the CT images |

MRFO: Manta ray foraging optimization, HGSO: Henry gas solubility optimization, HHO: Harris Hawks optimizer, GWO: Grey Wolf optimization, SCA: Sine cosine algorithm, WOA: Whale optimization algorithm, SMA: Slime Mould algorithm, PSO: Particle Swarm optimization, GA: Genetic algorithm, TTT: Toeplitz, GGG: Gaussian, CCC: Circulate

similar to the normal photographic film. Two types of computed tomography of the chest are available, high resolution computed tomography and spiral chest.[31] Corona's disease occurs on a CT scan of the chest in three signs: Ground vitreous appearance, circumferential distribution in the pleura and more than one center of infection in one case.

### X-ray (chest X-ray radiography [CXR])

CXR is a scrutiny in which electromagnetic rays produced from special radioactive equipment's to penetrating the body's tissues, and hit a plate placed behind the body. The main disadvantage of using CT imaging due to it is expense and delivers high radiation dose.[32] It is considered a very useful diagnostic tool for automatically testing COVID-19 features. Computer-assisted therapy is used for X-rays or chest CT images for a wide variety of diseases including osteoporosis,[33] cancer,[34] and heart disease[35] and in Hong Kong study.[36]

The main contribution of this paper is the scheduling of research papers according to the steps to complete their treatment to verify the distinction or drawback in each stage. The paper rest was organized as follows: In Sect. II, analysis of the research references in Tables 1 and 2. Sect. III concludes the paper.

## LITERATURE REVIEW

Since the emergence of the Coronavirus until now, many researchers have rushed to work on automatic diagnosis of the disease using imaging techniques for CXR and CT scan. All research involved the many steps needed for automatic detection of COVID-19 using image processing that includes the procedures shown in Figure 6. To clarify the contributions of many researchers, their papers were analyzed according to the treatment steps as shown in Table 1. And the advantage and disadvantages are listed in Table 2.

## DISCUSSION

Recently, deep learning of neural networks has played a prominent role in training very

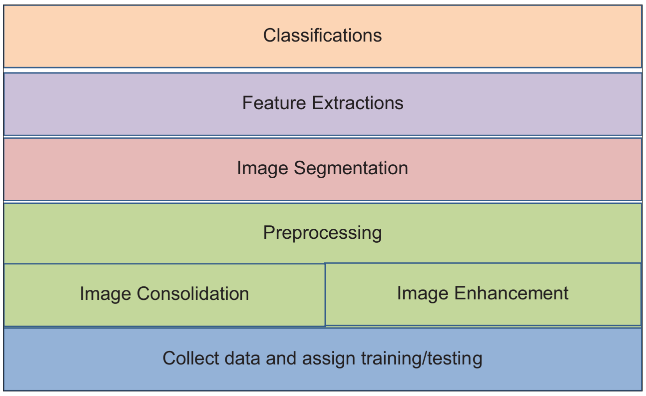


**Figure 6:** Classifications Image processing steps

**Table 3:** Constructive study of detection phases

| Phase | Discussion | Ref. |
|---|---|---|
| Datasets | 1- Data on Covid-19 is still sparse compared to other cases, like Pneumonia, Adenovirus, Norovirus, Orf, Papilloma, Rift Valley, Rotavirus, West Nile, SARS-CoV2, Astrovirus, CCHF, Cowpox, Dengue, Ebola, Inuenza, Lassa, Marburg, Normal<br>2-Most of the papers use X-ray images, a few use CT scans. There is no research to classify regardless of the type of images<br>3- Unavailability of a cut-out image of the classified part of the disease by specialists | [43]<br>[49]<br>[60]<br>[70]<br>[79]<br>[85]<br>[87]<br>[88] |
| Processing | 1. Many paper not doing any pre-processing procedure like resizing images, rotate some images to alignment them appearance at same manner<br>2. Most research not cut out unwanted parts of the images<br>3. Not making any improvement on most of the datasets images<br>4. Few papers have worked to reduce the dimensions of a large data set by using PCA | [57]<br>[79]<br>[82]<br>[87]<br>[88] |
| Segmentation | All images in most of the research are fully trained without deducing only the part that contains the disease characteristic | [37]<br>[49]<br>[52] |
| Features | Few papers talked about extracting features because they automatically extracted from images with a most recently researches by deep learning style flow | [40]<br>[49]<br>[52]<br>[70]<br>[73]<br>[82] |
| Classifications | Several new COVID-19 classification research papers have adopted by applying deep neural networks with multiple layers and data. Many models were used such as AlexNet, SqueezeNet, GoogleNet, various versions of the Visual Geometry Group(VGG), ResNet types, Xception, various types MobileNet, DenseNet, U-Net etc. Many papers classified images into COVID, not COVID, other distrusted on three classes, on the other hand[70] distinguishes data to 16 virus's classes | [49]<br>[54]<br>[70]<br>[79] |

large data, including CT and X-ray images, to diagnose Covid-19 and for various types of networks. The coherence of the five stages with each other is very important, so any slackness in any stage reduces the accuracy of classification. High accuracy does not come only by adopting the best in all stages. The discussion points of each phase are written in Table 3, with the best references for each stage.

## CONCLUSION

The novelty of this paper is to organize the reviewing research's depend on their processing stages to offering the needed in future work in each phase. In the first stage, a gap was observed in the COVID injuries images, especially in the primary papers, and with time this problem was covered, but it still needed to collect images of both types X-ray and CT classified by specialists. In the second stage most researches omission the pre-processing treatment, including standardizing the size of the images or rotating them in a way that all images become the same or cropped unwanted parts. As well as improving the images, which was included in only two researches. In third phase, most researches paper used deep learning which includes micro multi-layer perceptron's into the filters of convolutional layers to extract more complicated features so it not states in the most papers. For future work the main contribution can be done in fourth stage, to segment the COVID-19 lesion part from the images for better classification accuracy. All reviewing papers can be increasing their accuracies when training images after extracts lesion only from whole images. To improve the classification system, it is better to have the classification system free for any X-ray or CT images with add an analysis of the patient's cough sound simulating the doctor's work.

## ACKNOWLEDGMENTS

The authors would like to express their deep gratitude and thanks to the Department Computer Engineering-College of Engineering/University of Mosul for their support in this study.

## REFERENCES

1. World Health Organization. Novel Coronavirus (2019-nCoV) Situation Report-30. Geneva: World Health Organization; 2020. Available from: https://www.who.int/docs/default-source/coronaviruse/

situationreports/20200219-sitrep-30-covid-19.pdf?sfvrsn=6e50645_2.2020.
2. Available from: https://www.sehhty.com. Website health statistics to monitor globally documented cases of Covid-19, [Last accessed on 2020 Feb 23].
3. Available from: https://www.coronatracker.com/analytics. For CoronaTracke. [Last accessed on 2020 Jan 12].
4. Epidemiology Working Group for NCIP Epidemic Response, Chinese Center for Disease Control and Prevention. The epidemiological characteristics of an outbreak of 2019 novel coronavirus diseases (Covid-19) in China. Zhonghua Liu Xing Bing Xue Za Zhi 2020;41:145-51.
5. Xie Z. Pay attention to SARS-CoV-2 infection in children. Pediatr Invest 2020;4:1-4.
6. Wang D, Hu B, Hu C, Zhu F, Liu X, Zhang J, *et al*. Clinical characteristics of 138 hospitalized patients with 2019 novel coronavirus-infected pneumonia in Wuhan, China. JAMA 2020;323:1061-9.
7. Ai T, Yang Z, Hou H, Zhan C, Chen C, Lv W, *et al*. Correlation of chest CT and RT-PCR testing for coronavirus disease 2019 (COVID-19) in China. A report of 1014 cases. Radiology 2020;296:E32-40.
8. Xu X, Jiang X, Ma C, Du P, Li X, Lv S, *et al*. Deep learning system to screen coronavirus disease 2019 pneumonia. arXiv 2002;2002:09334.
9. Wang S, Kang B, Ma J, Zeng X, Xiao M, Guo J, *et al*. A deep learning algorithm using CT images to screen for Corona Virus Disease (COVID-19). medRxiv 2020;220:20023028.
10. Matta DM, Saraf MK. Prediction of COVID-19 Using Machine Learning Techniques. Karlskrona, Sweden: Faculty of Computing, Blekinge Institute of Technology; 2020. p. 79.
11. Jamshidi M, Lalbakhsh A, Talla J, Peroutka Z, Hadjilooei F, Lalbakhsh P, *et al*. Artificial intelligence and COVID-19: Deep learning approaches for diagnosis and treatment. Special section on emerging deep learning theories and methods for biomedical engineering. IEEE Access 2020;8:109581-95.
12. Rajasekaran S, Vijayalakshmi Pai GA. Neural Networks, Fuzzy Logic And Genetic Algorithms: Synthesis and Applications. New Delhi: PHI Learning Private Limited; 2013.
13. Zhu X, Rehman KU, Wang B, Shahzad M. Modern soft-sensing modeling methods for fermentation processes Sensors 2020;20:1771.
14. Dhiman N, Sharma MK. Diabetes diagnostic model based on truth-value restrictions method using inference of intuitionistic conditional and qualified fuzzy propositions. Int J Eng Adv Technol 2019;9:5015-21.
15. Dhiman N, Sharma MK. Mediative Sugeno's-TSK fuzzy logic based screening analysis to diagnosis of heart disease. Appl Math 2019;10:448-67.
16. Dhiman N, Sharma MK. Mediative multi-criteria decision support system for various alternatives based on fuzzy. Int J Recent Technol Eng 2019;8:7940-6.
17. Das S. CNN Architectures: LeNet, AlexNet, VGG, GoogLeNet, ResNetandmore, Medium; 2017. Available from: https://medium.com/analytics-vidhya/cnns-architectures-lenet-alexnet-vgg-googlenet-resnet-and-more-666091488df5 [Last accessed on 2020 Jan 19].
18. Zeng G, He Y, Yu Z, Yang X, Yang R, Zhanga L. Preparation of novel high copper ions removal membranes by embedding organosilane-functionalized multi-walled carbon nanotube. J Chem Technol Biotechnol 2016;91:2322-30.
19. Iandola FN, Han S, Moskewicz MW, Ashraf K, Dally WJ, Keutzer K. Squeezenet: AlexNet-level accuracy with 50x fewer parameters and <0.5MB model size. arXiv 2016;2016:7360.
20. Simonyan K, Zisserman A. Very deep convolutional networks for large-scale image recognition. arXiv 206;2016:7360.
21. Jafar A, Lee M. Hyperparameter Optimization for Deep Residual Learning in Image Classification. IEEE International Conference on Autonomic Computing and Self-Organizing Systems Companion (ACSOS-C); 2020. p. 24-9.
22. Chollet F. Xception: Deep Learning with Depthwise Separable Convolutions. IEEE Conference on Computer Vision and Pattern Recognition; 2017. p. 1800-7.
23. Szegedy C, Ioffe S, Vanhoucke V, Alemi A. Inception-v4, Inception-ResNet and the Impact of Residual Connections on Learning. Vol. 4. 31st The AAAI Conference on Artificial Intelligence; 2017.
24. Qin Z, Zhang Z, Chen X, Wang C, Peng Y. FD-MobileNet: Improved MobileNet with a Fast Down Sampling Strategy. Athens, Greece: 25th IEEE International Conference on Image Processing (ICIP); 2018. p. 1363-7.
25. Huang G, Liu Z, Van Maaten L, Weinberger KQ. Densely Connected Convolutional Networks. Honolulu, HI, USA: IEEE Conference on Computer Vision and Pattern Recognition (CVPR); 2017. p. 2261-9.
26. Ronneberger O, Fischer P, Brox T. U-Net: Convolutional Networks for Biomedical Image Segmentation. Switzerland: Springer International Publishing; 2015. p. 234-41.
27. Kerenidis I, Landman J, Prakash A. Quantum algorithms for deep convolutional neural networks. arXiv 2019;2019:1117.
28. Dong D, Tang Z, Wang S, Hui H, Gong L, Lu Y, *et al*. The role of imaging in the detection and management of covid-19: A review. IEEE Rev Biomed Eng 2021;14:16-29.
29. Li L, Qin L, Xu Z, Yin Y, Wang X, Kong B, *et al*. Using artificial intelligence to detect COVID-19 and community-acquired pneumonia based on pulmonary CT: Evaluation of the diagnostic accuracy. Radiology 2020;296:E65-71.
30. Shi F, Wang J, Shi J, Wu Z, Wang Q, Tang Z, *et al*. Review of artificial intelligence techniques in imaging data acquisition, segmentation and diagnosis for COVID-19. IEEE Rev Biomed Eng 2020;14:4-15.
31. Computed Tomography (CT)-Chest; 2020. Available from: https://www.radiologyinfo.org/en/info/chestct [Last accessed on 2020 Jan. 20].
32. Kroft LJ, der Velden LV, Girón IH, Roelofs JJ, de Roos A, Geleijns J. Added value of ultra-low-dose computed tomography, dose quivalent to chest X-ray

radiography, for diagnosing chest pathology. Thorac Imaging 2019;34:179-86.
33. Pisani P, Renna MD, Conversano F, Casciaro E, Muratore M, Quarta E, *et al*. Screening and early diagnosis of osteoporosis through X-ray and ultrasound based techniques. World J Radiol 2013;5:398-410.
34. Al-Antaria MA, Al-Masnia MA, Choib MT, Hana SM, Kima TS. A fully integrated computer-aided diagnosis system for digital X-ray mammograms via deep learning detection, segmentation, and classification. Int J Med Inf 2018;117:44-54.
35. Speide MA, Wilfley BP, Star-Lack JM, Heanue JA. Scanning-beam digital x-ray (SBDX) technology for interventional and diagnostic cardiac angiography. Med Phys 2006;33:2714-27.
36. Ming-Yen N, Elaine YP, Jin Y, Fangfang Y, Xia L, Hongxia W, *et al*. Imaging profile of the COVID-19 infection: Radiologic findings and literature review. Radiology 2020;2:e200034.
37. Gozes O, Frid-Adar M, Greenspan H, Browning PD, Zhang H, Ji W, *et al*. Rapid AI development cycle for the coronavirus (Covid-19) Pandemic: Initial results for automated detection and patient monitoring using deep learning CT image analysis. Radiology 2020;2020:22.
38. Chain Z. Available from: http://www.chainz.cn [Last accessed on 2020 Jan 14].
39. Sethy PK, Behera SK. Detection of coronavirus disease (Covid-19) based on deep features. Preprints 2020;2020:2020030300.
40. Barstugan M, Ozkaya U, Ozturk S. Coronavirus (COVID-19) classification using CT images by machine learning methods. arXiv 2003;2003:09424.
41. Narin A, Kaya CN, Pamuk ZT. Automatic detection of coronavirus disease (COVID-19) using X-ray images and deep convolutional neural networks. arXiv 2003;2003:10849.
42. Cohen JP, Morrison P, Dao L. Covid-19 image data collection. arXiv 2003;2003:11597.
43. Apostolopoulos ID, Mpesiana TA. Covid19: Automatic detection from Xray images utilizing transfer learning with convolutional neural networks. Phys Eng Sci Med 2002;43:635-40.
44. Cohen JP. Covid-19 Image Data Collection; 2020. Available from: https://www.github.com/ieee8023/covid-chestxray-dataset. [Last accessed on 2020 Feb 15].
45. Zisserman AS. Very deep convolutional networks for large-scale image recognition. arXiv 2015;2015:14091556.
46. Howard AG, Zhu M, Chen B, Kalenichenko D, Wang W, Weyand TS, *et al*. MobileNets: Efficient convolutional neural networks for mobile vision applications. arXiv 2017;2017:170404861.
47. Szegedy C, Ioffe S, Vanhoucke V, Alemi AA. Inception-v4, Inception-resnet and the Impact of Residual Connections on Learning. 31st AAAI Conference on Artificial Intelligence; 2017. p. 7.
48. Chollet F. Xception: Deep learning with depthwise separable convolutions. arXiv 2017;2017:161002357.
49. Xu X, Jiang X, Ma C, Du P, Li X, Lv S, *et al*. A deep learning system to screen novel coronavirus disease 2019 pneumonia. Engineering 2020;6:1122-9.
50. Milletari F, Navab N, Ahmadi S. V-Net: Fully convolutional neural networks for volumetric medical image segmentation. arXiv 2016;2016: 4797.
51. He K, Zhang X, Ren S, Sun J. Deep residual learning for image recognition. arXiv 2015;2015:3385.
52. Singh D, Kumar V, Vaishali, Kaur M. Classification of COVID-19 patients from chest CT images using multi-objective differential evolution-based convolutional neural networks. Eur J Clin Microbiol Infect Dis 2020;39:1379-89.
53. Gu J, Wang Z, Kuen J, Ma L, Shahroudy A, Shuai B, Liu T, *et al*. Recent advances in convolutional neural networks. arXiv 2017;2017:7108.
54. Togaçar M, Ergen B, CÖmert Z. Covid-19 detection using deep learning models to exploit Social Mimic Optimization and structured chest X-ray images using fuzzy color and stacking approaches. Comput Biol Med 2020;121:103805.
55. Cohen JP. Covid-19 Chest X-Ray dataset or CT dataset, GitHub; 2020. Available from: https://www.github.com/ieee8023/co vid-chestxray-dataset. [Last accessed on 2020 Mar 10].
56. Rahman T, Chowdhury M, Khandakar A. Covid-19 Radiography Database, Kaggle; 2020. Available from: https://www.kaggle.com/tawsifurrahman/covid19-radiography-database/data#. [last accessed on 2020 Apr 20].
57. Rahimzadeh M, Attar AA. Modified deep convolutional neural network for detecting covid-19 and Pneumonia from Chest X-Ray Images Based on the Concatenation of Xception and ResNet50V2. Inf Med Unlocked 2020;19:100360.
58. Available from: https://github.com/ieee8023/covid-chestxray-dataset. [Last accessed on 2020 Feb 09].
59. Available from: https://www.kaggle.com/c/rsnapneu monia-detection-challenge. [Last accessed on 2020 Feb 11].
60. Cohen JP, Dao L, Morrison P, Roth K, Bengio Y, Shen B, *et al*. Predicting COVID-19 pneumonia severity on chest X-ray with deep learning. arXiv 2005;2005:11856.
61. Shih G, Wu CC, Halabi SS, Kohli MD, Prevedello LM, Cook TS, *et al*. Augmenting the national institutes of health chest radiograph dataset with expert annotations of possible pneumonia. Radiograph 2019;1:e180041.
62. Irvin J, Rajpurkar P, Ko M, Yu Y, Ciurea-Ilcus S, Chute C, et al. CheXpert: A Large Chest Radiograph Dataset with Uncertainty Labels and Expert Comparison. The Thirty-Third AAAI Conference on Artificial Intelligence (AAAI-19); 2019. p. 590-7.
63. Wang X, Peng Y, Lu L, Lu Z, Bagheri M, Summers RM. ChestX-ray8: Hospital-Scale Chest X-ray Database and Benchmarks on Weakly-supervised Classification and Localization of Common Thorax Diseases. Computer Vision Foundation; 2017. p. 2097-106.
64. Majkowska A, Mittal S, Steiner DF, Reicher JJ, Kinney SM, Duggan GE, *et al*. Chest radiograph interpretation with deep learning models: Assessment with radiologist-adjudicated reference standards and population-adjusted evaluation. Radiology 2020;294:421-31.
65. Johnson AE, Pollard TJ, Greenbaum NR, Lungren MP, Deng C, Peng Y, *et al*. MIMIC-CXR-JPG, A

Large Publicly Available Database of Labeled Chest Radiographs. arXiv; 2019.
66. Bustos A, Pertusa A, Salinas J, Iglesia-Vayác M. PadChest: A large chest x-ray image dataset with multi-label annotated reports. Med Image Anal 2020;66:101797.
67. Demner-Fushman D, Kohli MD, Rosenman MB, Shooshan SE, Rodriguez L, Antani S, *et al*. Preparing a collection of radiology examinations for distribution and retrieval. J Am Med Inf Assoc 2016;23:304-10.
68. Huang G, Liu Z, van der Maaten L, Weinberger KQ. Densely Connected Convolutional Networks. Proceedings of the IEEE Conference on Computer Vision and Pattern Recognition (CVPR); 2017. p. 4700-8.
69. Panwar H, Gupta PK, Siddiqui MK, Morales-Menendez R, Singh V. Application of deep learning for fast detection of COVID-19 in X-Rays using nCOVnet. Chaos Solitons Fractals 2020;138:109944.
70. Dabiri Y, Kassab GS. Machine learning analysis of virus based on transmission electron microscopy images: Application to SARS-CoV-2; 2020. p. 17.
71. Kylberg G, Uppström M, Sintorn IM. Virus texture analysis using local binary patterns and radial density proles. In: Lecture Notes in Computer Science. Berlin, Heidelberg: Springer; 2011.
72. National Institute of Allergy and Infection diseases. Available from: https://www.niaid.nih.gov/news-events/novel-coronaviru s-sarscov2-images.
73. Abd Elaziz M, Hosny KM, Salah A, Darwish MM, Lu S, Sahlol AT. New machine learning method for imagebased diagnosis of COVID-19. PLoS One 2020;2020:0235187.
74. Andrea DA, Radiology COVID-19 Database. Available from: https://www.sirm.org/category/senza-categoria/covid-19. [Last accessed on 2020 Apr 11].
75. Civit-Masot J, Luna-Perejón F, Morales MD, Civit A. Deep learning system for COVID-19 diagnosis aid using X-ray pulmonaryimages. Appl Sci 2020;13:4640.
76. Available from:https://public.roboflow.com/classification/covid-19-and-pneumonia-scans [Last accessed on 2020 Mar 16].
77. Zulfaezal M, Azemin C, Hassan R, Tamr MI, Ali MA. Covid-19 deep learning prediction model using publicly available radiologist-adjudicated chest X-ray images as training data: Preliminary findings. Int J Biomed Imaging 2020;2020:8828855.
78. Available from: https://cloud.google.com/healthcare/docs/resources/public-datasets/nih-chest [Last accessed on 2020 Mar. 16].
79. Sekeroglu B, Ozsahin I. Detection of COVID-19 from chest X-ray images using convolutional neural networks. SLAS Technol 2020;25:553-65.
80. Kermany DS, Goldbaum M, Cai W, Valentim CS, Liang H, Baxter SL, *et al*. identifying medical diagnoses and treatable diseases by image-based deep learning. Cell 2018;172:1122-31.
81. Haralick RM, Shapiro LG. Computer and Robot Vision. Vol. 1. Boston, Massachusetts: Addison-Wesley; 1992. p. 346-51.
82. Abbas A, Abdelsamea MM, Gaber MM. Classification of Covid-19 in chest X-ray images using DeTraC deep convolutional neural network. Appl Intell 2020;2020:11.
83. Candemir S, Jaeger S, Palaniappan K, Musco JP, Singh RK, Xue Z, *et al*. Lung segmentation in chest radiographs using anatomical atlases with nonrigid registration. IEEE Trans Med Imaging 2014;33:557-90.
84. Jaeger S, Karargyris A, Candemir S, Folio L, Siegelman J, Callaghan F, *et al*. Automatic tuberculosis screening using chest radiographs. IEEE Trans Med Imaging 2014;33:233-45.
85. Sahlol AT, Yousri D, Ewees AA, Al-Qaness MA, Damasevicius R, Abd Elaziz M. Covid-19 image classifcation using deep features and fractionalorder marine predators algorithm. Sci Rep 2020;10:15364.
86. Rajpurkar P, Irvin J, Zhu K, Yang B, Mehta H, Duan T, *et al*. CheXNet: Radiologist-level pneumonia detection on chest X-rays with deep learning. arXiv 2017;2017:1711.
87. Jain R, Gupta M, Taneja S, Hemanth DJ. Deep learning based detection and analysis of Covid-19 on chest X-ray images. Appl Intell 2020;2020:11.
88. Wang L, Lin ZQ, Wong AR. Covid-net: A tailored deep convolutional neural network design for detection of COVID-19 cases from chest X-ray images. Sci Rep 2020;10:19549.
89. Chung, A. Figure 1 Covid-19 Chest x-Ray Data Initiative; 2020. Available from: https://github.com/agchung/Figure1-COVID-chestxray-dataset. [Last accessed on 2020 Feb 16].
90. Radiological Society of North America. RSNA Pneumonia Detection Challenge; 2019. Available from: https://www.kaggle.com/c/rsna-pneumonia-detection-challe-nge/data. [Last accessed on 2020 Jan 13].
91. Chung, A. Actualmed COVID-19 Chest x-ray Data Initiative; 2020. Available from: https://www.github.com/agchung/Actual med-Covid-chestxray-dataset. [Last accessed on 2020 Feb 11].
92. Radiological Society of North America. COVID-19 Radiography Database; 2019. Available from: https://www.kaggle.com/tawsifurrahman/covid19-radiography-database. [Last accessed on 2020 Mar 12].
93. Awedat K, Essa A. Covid-CLNet: Covid-19 detection with compressive deep learning approaches. arXiv 2012;2021:2234.
94. RADLogics Inc. Available from: http://www.radlogics.com. [Last accessed on 2020 Jan 09].